

# Producing directed migration with correlated atoms in a tilted ac-driven lattice

Yi Zheng<sup>1</sup> and Shi-Jie Yang<sup>1,2,\*</sup>

<sup>1</sup>*Department of Physics, Beijing Normal University, Beijing 100875, China*

<sup>2</sup>*State Key Laboratory of Theoretical Physics, Institute of Theoretical Physics, Chinese Academy of Sciences, Beijing 100190, China*

(Received 26 February 2016; published 7 June 2016)

The correlated atoms in a tilted optical lattice driven by an ac field are studied within the Hubbard model. By making use of both photon-assisted tunneling and coherent destructive tunneling effects, we can move a pair of strongly correlated atoms in the lattice via manipulating the global amplitude of the driving field. We propose a scheme for creating entanglement between the particle pair and a single particle through interacting oscillations. Our model may provide a new building block for investigating quantum computing and quantum information processing with ultracold atoms in optical lattices.

DOI: [10.1103/PhysRevA.93.063609](https://doi.org/10.1103/PhysRevA.93.063609)

## I. INTRODUCTION

The high level of controllability and cleanness of ultracold quantum gases in optical lattices has enabled the simulation and exploration of fundamental many-body physics [1,2]. In experiments, the progress in detecting techniques has reached the single-site resolution level with high fidelity [3–5]. Many theoretical models, such as the tight-binding Hubbard models [6–9] and the Harper Hamiltonian with artificial gauge fields [10,11], are now experimentally achievable. In these systems, significant phenomena were demonstrated, including the basic superfluid-Mott insulator (MI) transition [7], (fractional) quantum Hall effects [12–15], etc.

The accurate manipulating and engineering schemes of such systems are the major tasks that require further investigation. The celebrated Bloch oscillations (BOs) are one of the direct quantum controls of a wave packet moving in a tilted lattice [16]. On the other hand, a periodically driving field can lead to photon-assisted tunneling [17], dynamical localization [18,19], and coherent destruction of tunneling (CDT) [20–23], etc. [24–26]. These effects provide potential applications for quantum control and give a better understanding of the solid-state physics. Recently, an induced effective gauge field based on the Floquet theory was considered for the study of topological effects [27–29]. The control of single-particle tunneling was proposed in Ref. [30] where the bipartite superlattices were modulated periodically to induce the directed CDT. Two-particle entanglement can also be realized in such systems. The interaction between particles has novel effects on the dynamics [31–33]. Research on the correlations has led to some specific phenomena, such as the coherent transport [25,34,35] and BOs with fractional Bloch periods [36,37].

In a previous paper, we have investigated the directed migration of a pair of strongly correlated atoms in optical lattices driven by doubly modulated ac fields [38]. In this paper we demonstrate the migration of a correlated particle pair in a one-dimensional (1D) tilted optical lattice driving by a modulated ac field. This scheme may be more experimentally feasible [17] in comparison to directly manipulating the on-site interaction through the Feshbach resonance [39,40]. The relevant factors in our scheme include renormalization of the hopping

amplitude, photon-assisted tunneling, as well as CDT. The time evolutions of the correlated pair are simulated by applying the Schrödinger equation with the time-dependent Hamiltonian. We propose a scheme for creating entanglement between the interacting atoms in the driven lattice which may find potential applications in quantum computing and engineering.

The paper is organized as follows. In Sec. II we describe the driving system within the Bose-Hubbard model and derive the effective hopping. The migration scheme and a bifurcating quantum motion are presented in Sec. III. In Sec. IV, we show the mixing and separating of a (2+1)-particle system via properly modulating the driving field, which creates entanglement between a single particle and a particle pair. A summary is included in Sec. V.

## II. FORMULISM

We first consider two interacting particles in a 1D tilted lattice by applying a dc field and an adjustable ac field. Within the tight-binding approximation, the dynamics of the particles is described in the framework of the Bose-Hubbard model,

$$\hat{H} = -J \sum_j (\hat{b}_j^\dagger \hat{b}_{j+1} + \text{H.c.}) + \frac{U}{2} \sum_j \hat{n}_j (\hat{n}_j - 1) + K(t) \sum_j j \times \hat{n}_j, \quad (1)$$

where  $\hat{b}_j^\dagger$  ( $\hat{b}_j$ ) are the bosonic creation (annihilation) operators and  $\hat{n}_j = \hat{b}_j^\dagger \hat{b}_j$  are the number operators acting on site  $j$ . Parameters  $J, U$  are the nearest-hopping rate and the on-site interaction, respectively. The quantity  $K(t) = K_0 + K_1 \cos(\omega t)$  in the last term contains the dc-ac field with  $K_0, K_1$  as the amplitudes and  $\omega$  as the driving frequency. The  $K_0$  term can be acquired by applying a magnetic gradient along the lattice, and the  $K_1$  term can be acquired by periodically shifting the mirror which is used to form the standing waves. For weak interaction and small tilting, a high-frequency oscillation can lead to the standard renormalization of the hopping rates [41]. As the tilting is increased until  $K_0 = n\omega$  with  $n$  as an integer, we will expect the photon-assisted tunneling effects [17,42]. For strong interaction cases, the two particles occupying the same site form a bound pair, which undergoes correlated quantum walks or fractional BO in different situations [33,36].

\*Corresponding author: yangshijie@tsinghua.org.cn

We consider two identical bosons in the model and assume a strong interaction and a large tilting, i.e.,  $U \sim K_0 \sim \omega \gg J$ . The effective dynamics can be derived by applying Floquet theory in the high-frequency limit. In particular we are concerned with the specific conditions in the present paper:  $U = (N + \frac{1}{2})\omega$ ,  $K_0 = (M + \frac{1}{2})\omega$  with  $N$  and  $M$  integers. With  $\omega \gg J$ ,

$$\begin{aligned} U - K_0 &= (N - M)\omega \\ &\equiv \mu\omega, \\ U + K_0 &= (N + M + 1)\omega \\ &\equiv \nu\omega. \end{aligned} \quad (2)$$

The term  $\omega/2$  in  $K_0$  is significant since it suppresses the tunneling of an isolated particle to a neighboring empty site. The equal form of  $U$  ensures  $(U \pm K_0)/\omega$  to be integers, which means that the tunneling processes assisted with other particles are possible. The dynamical properties of these conditions will be discussed later. The two-particle state is represented in the Fock basis as  $|\Phi(t)\rangle = \sum_{n,m} c_{n,m} \hat{b}_n^\dagger \hat{b}_m^\dagger |0\rangle$ , where coefficients  $c_{n,m}$  are the probability amplitudes. This expansion contains a Bose enhancement factor of  $\sqrt{2}$  when  $n = m$ . By applying Schrödinger's equation of motion  $i \partial_t |\Phi(t)\rangle = \hat{H} |\Phi(t)\rangle$  ( $\hbar = 1$ ), one obtains the temporal evolution of  $c_{n,m}$ ,

$$i \frac{d}{dt} c_{n,m} = -J \sum_{\sigma=\pm 1} (c_{n+\sigma,m} + c_{n,m+\sigma}) + F_{n,m}(t) c_{n,m}, \quad (3)$$

where  $F_{n,m}(t) = U\delta_{n,m} + K(t)(n+m)$ . For two fermions with distinct spin states, the deduction can be performed in a similar manner within the Fermi-Hubbard model [43]. To employ the rotating-wave approximation and drop the trivial terms in the oscillation, we rewrite the amplitudes  $c_{n,m}(t)$  in terms of  $a_{n,m}(t)$  as

$$c_{n,m}(t) = a_{n,m}(t) \exp \left[ -i \int_0^t dt' F_{n,m}(t') \right]. \quad (4)$$

From Eqs. (3) and (4), we obtain the equation of motion for  $a_{n,m}(t)$ ,

$$\begin{aligned} i \frac{d}{dt} a_{n,m} &= -J \{ a_{n+1,m} \exp [iU(\delta_{n,m} - \delta_{n+1,m})t - iF(t)] \\ &\quad + a_{n,m+1} \exp [iU(\delta_{n,m} - \delta_{n,m+1})t - iF(t)] \\ &\quad + a_{n-1,m} \exp [iU(\delta_{n,m} - \delta_{n-1,m})t + iF(t)] \\ &\quad + a_{n,m-1} \exp [iU(\delta_{n,m} - \delta_{n,m-1})t + iF(t)] \}, \end{aligned} \quad (5)$$

where  $F(t) = K_0 t + K_1/\omega \sin(\omega t)$ . The standard renormalization procedure allows one to replace the fast oscillating terms with their averages over a period. Taking account of the conditions (2), the renormalized coupling amplitudes for  $|n-m| > 1$  vanish

$$\frac{1}{T} \int_0^T dt' \exp \left\{ \pm i \left[ K_0 t' + \frac{K_1}{\omega} \sin(\omega t') \right] \right\} = 0. \quad (6)$$

Note that Eq. (6) holds in the high-frequency limit due to the additional term  $\omega/2$  in  $K_0$ .

In order to put the initial expansion of  $|\Phi(t)\rangle$  in a more compact form, i.e.,  $|\Phi(t)\rangle = \sum_{n < m} c_{n,m} \hat{b}_n^\dagger \hat{b}_m^\dagger |0\rangle + \sum_n c_{n,n} |2\rangle_n$ ,

where  $|2\rangle_n$  indicates a double occupation on site  $n$ , we perform a substitution for each  $a_{n,m}$ :

$$\begin{aligned} (1) \quad a_{n,n} &\rightarrow \frac{1}{\sqrt{2}} a_{n,n}, \\ (2) \quad a_{n,m > n} &\rightarrow \frac{1}{2} a_{n,m > n}, \\ (3) \quad a_{n,m < n} &\rightarrow \frac{1}{2} a_{m < n,n}. \end{aligned}$$

Further calculations yield

$$\begin{aligned} i \frac{d}{dt} a_{n,n} &= -\sqrt{2} J_1 a_{n,n+1} - \sqrt{2} J_2 a_{n-1,n}, \\ i \frac{d}{dt} a_{n,n+1} &= -\sqrt{2} J_1 a_{n,n} - \sqrt{2} J_2 a_{n+1,n+1}, \\ i \frac{d}{dt} a_{n,m} &= 0 \quad (|n-m| > 1), \end{aligned} \quad (7)$$

where the hopping amplitudes have been renormalized as

$$J_1 = J \mathcal{J}_\mu \left( \frac{K_1}{\omega} \right), \quad J_2 = (-1)^\nu J \mathcal{J}_\nu \left( \frac{K_1}{\omega} \right), \quad (8)$$

with  $\mathcal{J}_\mu$  as the  $\mu$ th Bessel function of the first kind. These hopping amplitudes result from the restricted forms of  $U$  and  $K_0$ . We mention that Eqs. (7) can also be derived from a many-particle system in which one needs to expand the quantum state in the Fock basis labeled by  $|k\rangle \in \{|n_1^{(k)}, n_2^{(k)}, \dots, n_N^{(k)}\rangle\}$ . A similar deduction within conditions  $U, K_0 = m\omega/2$  (with  $m$  as an integer),  $\omega \gg J$  leads to an effective Hamiltonian with occupation-dependent hopping terms [44],

$$\hat{H}_{\text{eff}} = - \sum_{(i,j)} \hat{b}_i^\dagger J_{\text{eff}}(\hat{n}_i, \hat{n}_j) \hat{b}_j. \quad (9)$$

Explicitly, the tunneling channels between sites  $j$  and  $j+1$  with initial occupations  $n_j$  and  $n_{j+1}$ , respectively, have the effective hopping rates,

$$\begin{aligned} J_{(n_j, n_{j+1}) \rightarrow (n_{j+1}, n_{j+1}-1)} &= \begin{cases} J \mathcal{J}_{n_+} \left( \frac{K_1}{\omega} \right), & n_+ \in Z; \\ 0, & \text{otherwise,} \end{cases} \\ J_{(n_j, n_{j+1}) \rightarrow (n_{j-1}, n_{j+1}+1)} &= \begin{cases} J \mathcal{J}_{n_-} \left( \frac{K_1}{\omega} \right), & n_- \in Z; \\ 0, & \text{otherwise,} \end{cases} \\ n_\pm &= (n_j - n_{j+1} \pm 1) \frac{U}{\omega} - \frac{K_0}{\omega}, \end{aligned} \quad (10)$$

where  $Z$  represents the integer set. Applying Eqs. (10) to a two-particle system and restricting conditions (2), the effective tunnelings recover the dynamics described by Eq. (7) with the hopping rates reducing to  $J_1$  and  $J_2$ . A small deviation from the ‘‘resonant’’ conditions (2) will lead to a residual on-site Hubbard energy or a small lattice tilting [43]. In the MI regime with  $K_0 = 0$ , tuning the driving frequency resonant with the on-site interaction can lead to the destruction of the MI state as shown in Ref. [45]. It is notable that the on-site interaction is not required to be positive. Thus our model is equivalently applicable to attractive particles.

### III. MIGRATION OF A CORRELATED PAIR

For the correlated particle-pair model, Eqs. (7) indicate that all possible tunneling channels are

$$|2, 0\rangle_{j,j+1} \overset{A}{\leftrightarrow} |1, 1\rangle_{j,j+1} \overset{B}{\leftrightarrow} |0, 2\rangle_{j,j+1}, \quad (11)$$

where the channels labeled by  $A$  and  $B$  have hopping rates  $J_1$  and  $J_2$ , respectively. The tunneling of an isolated particle is forbidden. Such tunneling properties stem from the conditions  $U = (N + \frac{1}{2})\omega$  and  $K_0 = (M + \frac{1}{2})\omega$ . Multiples of the energy quanta  $\omega$  ( $\hbar = 1$ ) which are provided by the periodically driving can compensate the energy cost from both the on-site interaction and the lattice tilting. However, the compensation cannot be distributed independently. The difference in the leftward and the rightward tunnelings is a consequence of the broken mirror symmetry that is induced by the tilting field.

We call the double occupation state, such as  $|2,0\rangle_{j,j+1}$ , the doublon and the state with one-particle occupation on nearest-neighboring sites, such as  $|1,1\rangle_{j,j+1}$ , the dimer. The variable amplitudes  $K_1$  make the tunneling rates  $J_1$  and  $J_2$  adjustable. Without losing the generality, we take a specific case of  $N = M = 0$  hereafter so that  $U = K_0 = \omega/2$ ,  $\mu = 0$ , and  $\nu = 1$ . By setting the oscillating amplitude  $K_1$  to  $\mathcal{J}_0(K_1/\omega) = 0$  or  $\mathcal{J}_1(K_1/\omega) = 0$ , we arrive at the CDT and thus obtain an oscillation between the doublon and the dimer state, namely,

$$(A) |2,0\rangle_{j,j+1} \leftrightarrow |1,1\rangle_{j,j+1}, \text{ as } \mathcal{J}_1(K_1^A/\omega) = 0,$$

$$(B) |1,1\rangle_{j,j+1} \leftrightarrow |0,2\rangle_{j,j+1}, \text{ as } \mathcal{J}_0(K_1^B/\omega) = 0.$$

The effective hopping rates are determined by  $J_{\text{res}}^A = J\mathcal{J}_0(K_1^A/\omega)$  and  $J_{\text{res}}^B = J\mathcal{J}_1(K_1^B/\omega)$ . Thus frequencies of the sinusoidal doublon-dimer oscillations  $A$  and  $B$  are  $\omega_{\text{osc}}^A = \sqrt{2}J_{\text{res}}^A$  and  $\omega_{\text{osc}}^B = \sqrt{2}J_{\text{res}}^B$ .

To verify the complete doublon-dimer oscillations, we carry out the numerical simulation of real-time evolution using the time-dependent Hamiltonian. The density distributions in Figs. 1(a) and 1(c) show the local oscillation with  $U = K_0 = \omega/2 = 20$  (in units of  $J$ ). We have set  $K_1^A/\omega = 3.8317$  in Figs. 1(a) and 1(b) and  $K_1^B/\omega = 2.4048$  in Figs. 1(c) and 1(d), which correspond to the oscillations  $A$  and  $B$ , respectively. The evolutions of the probability  $|\langle\Phi(t)|\text{doublon}(\text{dimer})\rangle|^2$  are shown in Figs. 1(b) and 1(d), which indicate the expected oscillations with different periods  $\pi/\omega_{\text{osc}}^A$  and  $\pi/\omega_{\text{osc}}^B$ . The analytical results from the effective model shown by squares in Figs. 1(b) and 1(d) are in good agreement with the direct simulation results.

By combining the  $A, B$  processes, we can arrive at the directed migration of the correlated particle pair as shown in Figs. 2(a) and 2(c). The driving amplitude  $K_1$  is properly modulated for the correlated pair to realize the series of hopping processes,

$$|2,0\rangle_{j,j+1} \rightarrow |1,1\rangle_{j,j+1} \rightarrow |0,2\rangle_{j,j+1},$$

which fulfill a complete cycle of migrating the doublon from site  $j$  to  $j + 1$ . We have set the period  $T_{A(B)} = \pi/2\omega_{\text{osc}}^{A(B)}$  for  $K_1 = K_1^{A(B)}$  as demonstrated in Figs. 2(b) and 2(d). The direction of motion can be well controlled by the modulation.

We note that the direction of migration also depends on whether the pair is initially a doublon or a dimer. By making use of this feature, one can achieve a bifurcating quantum motion by halving one of the time durations  $T_A$  (or  $T_B$ ). As shown in Fig. 3, by shortening the first  $T_B$  to its half, the oscillation  $B$  is incomplete, and the pair state becomes a superposition of  $|\text{doublon}\rangle$  and  $|\text{dimer}\rangle$ , i.e.,  $|\Psi\rangle = 1/\sqrt{2}|1,1\rangle_{7,8} + 1/\sqrt{2}|0,2\rangle_{7,8}$ . The state then propagates in two branches which move oppositely. If we halve the third

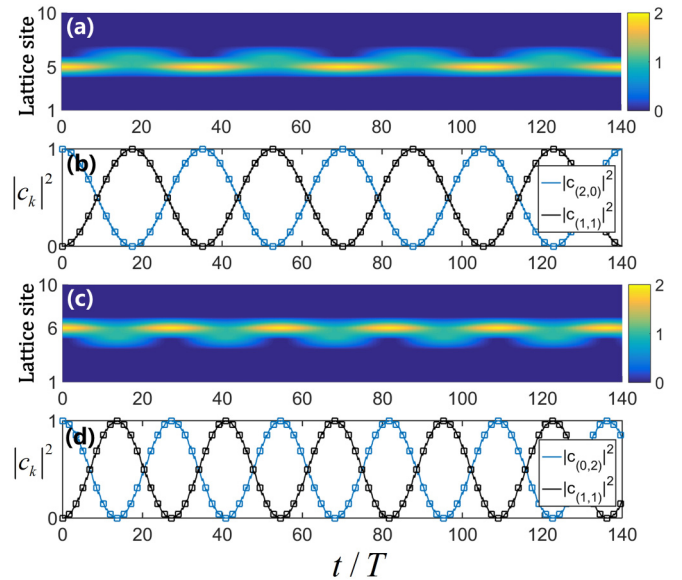


FIG. 1. Doublon-dimer oscillations (a) and (b) between states  $|0,2\rangle_{5,6}$  and  $|1,1\rangle_{5,6}$  and (c) and (d) between states  $|2,0\rangle_{5,6}$  and  $|1,1\rangle_{5,6}$ . The evolutions of density distribution are shown in (a) and (c), respectively, with driving amplitudes  $K_1/\omega = K_1^A/\omega = 3.8317$  and  $K_1/\omega = K_1^B/\omega = 2.4048$ . (b) and (d), respectively, are the temporal evolutions of the probability of the dimer state (black curves) and the doublon state (blue curves) with the probability labeled by  $|c_{(n_1,n_2)}|^2 = |\langle\Phi|n_1,n_2\rangle_{j,j+1}|^2$ . Analytical results from the effective model [Eq. (9)] are denoted by the squares.

$T_A$ , then the a further bifurcation occurs which results in four branches. This mechanism can serve as a quantum beam splitter that divides the correlated particle pair into coherent parts that propagate oppositely.

The proposed particle-pair migration scheme could be experimentally observed. The periodically driving Hubbard model with tilting in our consideration has been realized with cold atoms in optical lattices [17,46,47]. The parameters are highly controllable and can vary in a wide range. In these experiments with ultracold rubidium atoms, the magnitude of nearest-hopping rate  $J$  and on-site interaction  $U$  are tuned to

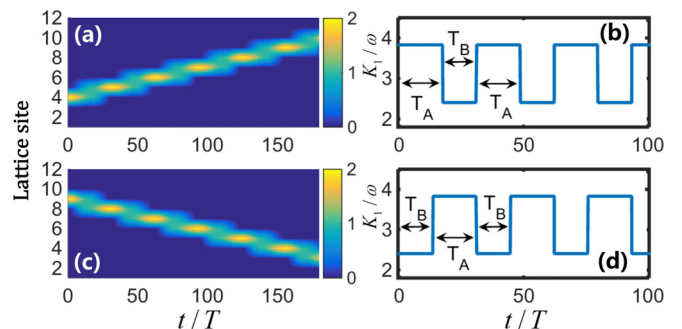


FIG. 2. (a) and (c) Directed migration of the correlated pair realized by the doublon-dimer oscillations shown in Fig. 1(a) and 1(c). (b) and (d) are the corresponding amplitude modulations of the driving field, respectively. We set  $K_1/\omega = K_1^A/\omega = 3.8317$  in the time-interval  $T_A$  and  $K_1/\omega = K_1^B/\omega = 2.4048$  in the time-interval  $T_B$ .

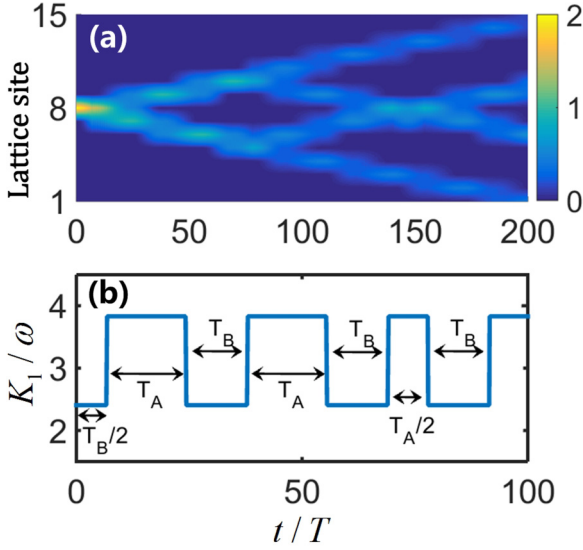


FIG. 3. (a) A bifurcating quantum motion realized by properly setting duration of the amplitude modulation as shown in (b). The variation of modulation leads to incomplete transition of the oscillations shown in Fig. 1, which results in the coexistence of the doublon and dimer.

$J/\hbar \sim 1$  kHz,  $J/U \sim 0.2$  [46], the value of driving amplitude  $K_1$  is tuned up to  $4\hbar\omega$  [47], and the lattice tilting can be arranged as  $K_0 \sim n\omega$  [17]. We will consider the driving frequency to fit the high-frequency limit with magnitude  $\omega \sim 40$  kHz. The hopping rate  $J$  decreases drastically with the increase in lattice depth, making it possible to reach the conditions in this paper.

#### IV. CREATING ENTANGLEMENT WITH THREE PARTICLES

One of the advantages of the driving schemes under conditions (2) is that an isolated particle is forbidden from tunneling to its adjacent sites whereas the correlated pair can make directed migration via properly modulating that driving field. Based on this consideration, we can realize a scattering process between a single particle and the particle pair. We first consider three identical particles, one isolated and two in a pair, which initially stay apart. Under the driving field the correlated pair moves toward the motionless single particle and mixes with it as shown in Fig. 4. The isolated particle can only tunnel to neighbor sites with the assistance of other particles. The modulation of driving amplitude is the same as that in Fig. 2(d) before state  $|102\rangle_{(4-6)}$  is formed at time  $3(T_A + T_B)$ . The further dynamics of the three particles can be elusive without restriction. However, while setting  $K_1 = K_1^B$ , all possible tunneling processes reduce to

$$|102\rangle_{(i,j,k)} \leftrightarrow |111\rangle_{(i,j,k)} \leftrightarrow |021\rangle_{(i,j,k)}, \quad (12)$$

where  $\langle i,j,k \rangle$  represents three neighboring sites  $i,j,k$  and  $|n_i, n_j, n_k\rangle$  as the state with  $n_i, n_j, n_k$  particles on sites  $i,j,k$ , respectively. All hopping rates are the same  $\tilde{J} = J\mathcal{J}_1(K_1^A/\omega)$ .

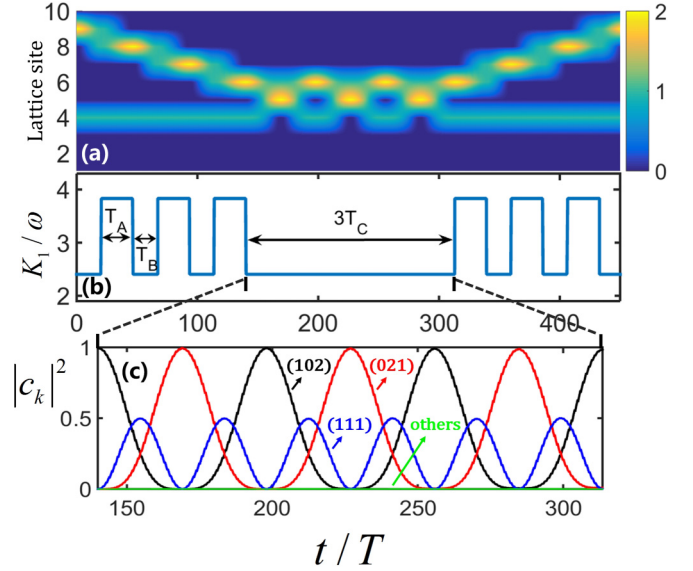


FIG. 4. A (2+1)-particle migration scheme. The isolated particle remains motionless whereas the correlated pair moves toward and mixes with the single particle. After that the particles separate. (a) The density evolution reveals the approaching, oscillating, and separating processes. (b) Modulations of the driving field with the amplitude between  $K_1^A/\omega$  and  $K_1^B/\omega$ . (c) The probability of the mixing three states  $|102\rangle_{(4,5,6)}$  (black),  $|111\rangle_{(4,5,6)}$  (blue), and  $|021\rangle_{(4,5,6)}$  (red) in the time-interval  $3T_C$  of (b). The green line indicates that the probability of other states, such as  $|c_{(120)}|^2$  and  $|c_{(201)}|^2$ , are severely damped.

Expanding the three-particle state by

$$|\Phi(t)\rangle = c_1(t)|102\rangle_{(i,j,k)} + c_2(t)|111\rangle_{(i,j,k)} + c_3(t)|021\rangle_{(i,j,k)},$$

the analytical results while assuming  $c_1(0) = 1$  are

$$\begin{aligned} c_1(t) &= \frac{1}{2} \cos(2\tilde{J}t) + \frac{1}{2}, \\ c_2(t) &= -\frac{i}{\sqrt{2}} \sin(2\tilde{J}t), \\ c_3(t) &= \frac{1}{2} \cos(2\tilde{J}t) - \frac{1}{2}. \end{aligned} \quad (13)$$

These formulas are consistent with the numerical results shown in Figs. 4(a) and 4(c). The oscillation periods are  $T_C = \pi/\tilde{J}$  for both  $|c_1(t)|^2$  and  $|c_3(t)|^2$  and  $T_C/2$  for  $|c_2(t)|^2$ . We have set  $K_1 = K_1^B$  for  $3T_C$  as shown in Fig. 4(b). The oscillation will recover the initial  $|102\rangle_{(4-6)}$  state at time  $3(T_A + T_B + T_C)$ . Thus a reverse modulation can be applied to separate the three particles into a pair and an isolated one.

Based on this knowledge, we are able to realize quantum entanglement by considering distinguishable particles. Now we assume the migrating particle pair to be  $a$ -type atoms and the single-particle  $b$ -type atom.  $a, b$  atoms can be a neutron boson of different hyperfine states. We label the particle-pair system  $A$  and the isolated single-particle system  $B$ , which are schematically illustrated in Fig. 5(a), thus  $|\Phi\rangle \in \mathcal{H}_A \otimes \mathcal{H}_B$ . The migrating (I), mixing (II), and separating (III) processes are similar to the identical particle case [Fig. 4(a)]. The modulation of the driving field is the same as that in Fig. 4(b).

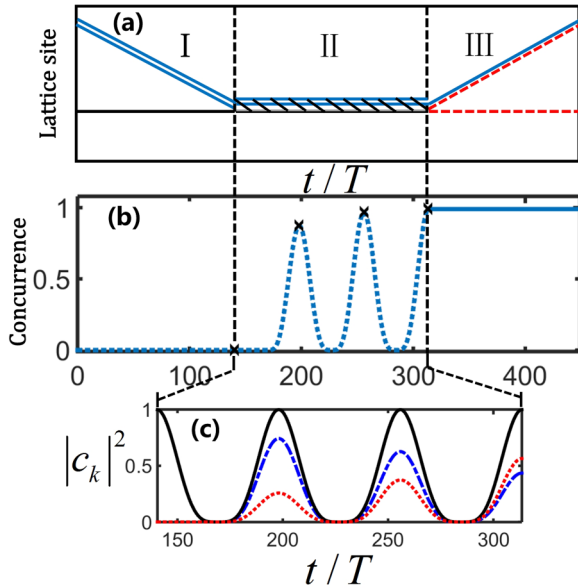


FIG. 5. (a) A schematic of the realization of entanglement with correlated particles in the driving lattice. The correlated pair of  $a$  atoms (blue double lines) moves toward a single  $b$  atom (black line) in time-interval I. After mixing in time-interval II, the separating particles are entangled in time-interval III. The dashed (red) lines indicate either  $a$  atom or  $b$  atoms. The double lines denote the correlated particle pair. (b) The evolution of the concurrences of the system. In II the concurrence is not well defined due to the full mixing of the three particles (plotted on the dotted curve) except those values marked by the crosses. In our case, we hold the oscillation for three periods, resulting in a large concurrence in III. (c) Numerical results in II starting from state  $|0\rangle_A \otimes |1\rangle_B = |aa\rangle_A \otimes |b\rangle_B$ , which belongs to  $|102\rangle_{(4-6)}$ . The probability evolution of state  $|102\rangle_{(4-6)}$  ( $|c_{102}|^2$ ) and its internal states  $|0\rangle_A \otimes |1\rangle_B = |aa\rangle_A \otimes |b\rangle_B$  ( $|c_{102}c_\alpha|^2$ ),  $|1\rangle_A \otimes |0\rangle_B = |ab\rangle_A \otimes |a\rangle_B$  ( $|c_{102}c_\beta|^2$ ) are shown by the black solid, blue dashed, and red dotted curves, respectively.

Regime I indicates the process of incidence of system  $A$  (the correlated  $a$ -atom pair) to the motionless system  $B$  (the isolated  $b$  atom). We label the initial state  $|aa\rangle_A \otimes |b\rangle_B$ , where  $|aa\rangle$  means that two particles in  $A$  are of type  $a$ . Regime II indicates the mixing regime with various oscillations. By setting the time duration in regime II to be multiples of  $T_C$ , we are able to subsequently separate the three particles into a bipartite system (regime III) of site-resolved  $A$  and  $B$ .

In general, the states before the incidence and after the mixing oscillations can be defined by

$$|\Phi\rangle_{AB} \in \{|aa\rangle \equiv |0\rangle, \quad |ab\rangle \equiv |1\rangle\}_A \otimes \{|a\rangle \equiv |0\rangle, \\ |b\rangle \equiv |1\rangle\}_B,$$

where  $|ab\rangle$  means finding one particle to be of type  $b$  in system  $A$ . The separating process (III) after the three-particle mixing oscillations starts from state  $|\Phi\rangle = |102\rangle_{4-6}$ . To give insight into the internal states, we perform a decomposition  $|102\rangle_{4-6} = c_\alpha|0\rangle_A \otimes |1\rangle_B + c_\beta|1\rangle_A \otimes |0\rangle_B$  with normalization condition  $|c_\alpha|^2 + |c_\beta|^2 = 1$ . A simulation has been carried out for the oscillation regime II. In Fig. 5(c), we show the probability of states  $|102\rangle_{4-6}$  ( $|c_{102}|^2$ , the black real curve),  $|0\rangle_A \otimes$

$|1\rangle_B$  ( $|c_{102}c_\alpha|^2$ , the blue dashed curve), and  $|1\rangle_A \otimes |0\rangle_B$  ( $|c_{102}c_\beta|^2$ , the red dashed curve). The oscillation of  $|c_{102}|^2$  (the black curve) in Fig. 5(c) is identical to that in Fig. 4(c). In regime III the two branches form an entangled state, and the degree of entanglement for a two-partite system is measured by the concurrence  $C(\Phi_{AB})$  [48], which is defined by

$$C(\Phi_{AB}) = 2|c_{00}c_{11} - c_{01}c_{10}|, \quad (14)$$

with  $\{c_{00}, c_{11}, c_{01}, c_{10}\}$  as the coefficients of state  $|\Phi_{AB}\rangle$ . A two-partite system is maximally entangled when  $C = 1$ , e.g., the two-qubit Bell states, such as  $1/\sqrt{2} \times (|01\rangle \pm |10\rangle)$ , whereas  $C = 0$  indicates the factorizability of the two-partite wave function. In our case the concurrence can be calculated through  $C = 2|c_\alpha c_\beta|$ . Note that the final state in Fig. 4 depends on the ending point of the three-particle oscillation with time duration  $\tilde{T} = nT_C$ ,  $n = 0, 2, \dots$ . The concurrence of the system with site-resolved two parts  $A, B$  depends on discrete  $n$ . Four possible values of  $C(n)$  are marked by the crosses in Fig. 5(b). At the beginning of the oscillation, we have  $C = 0$  showing no entanglement, which is also true before mixing of the two parts  $A$  and  $B$ . After a duration of mixing  $\tilde{T} = 3T_C$ , we reach a large entanglement state with  $C \approx 0.99$ . This state is stable and detectable in the lattice system. With increasing  $n$ , concurrence approaches  $2\sqrt{2}/3$  since  $|c_{102}|^2 = 1$  and  $|c_\alpha|^2 \rightarrow 1/3$ ,  $|c_\beta|^2 \rightarrow 2/3$ . In the separating procedure after oscillating with a large  $n$ , the  $A$  part of the particle pair evolves between the doublon and the dimer. When the dimer is formed from state  $|1\rangle_A = |ab\rangle_A$ , the probabilities of finding states  $|a, b\rangle_{(i,j)}$  and  $|b, a\rangle_{(i,j)}$  are equal. By regarding the three particles as a site-resolved tripartite system, we can arrive at the entangled three-qubit states, e.g.,

$$|\Phi\rangle = \frac{1}{\sqrt{3}}(|b, a, a\rangle_{i,j,j+1} + |a, b, a\rangle_{i,j,j+1} + |a, a, b\rangle_{i,j,j+1}), \quad (15)$$

which can be intuitively represented by the specific state  $|W\rangle = 1/\sqrt{3} \times (|100\rangle + |010\rangle + |001\rangle)$ . The  $|W\rangle$  state represents the south pole of a Bloch sphere for the two-dimensional space, whereas the north pole is represented by the orthogonal Greenberger-Horne-Zeilinger state [49].

Since the entanglement has been built at the end of the interacting oscillation and subsequent modulations of the particle pair are available, we arrive at a quantum gate controlled by global modulations of the lattice. The capabilities of parallel processing in this model indicate possible applications on the further research of multiparticle entangled states.

## V. SUMMARY

We have investigated correlated atoms in a driving Hubbard model. We focus on fast driving, strong interaction, and a large tilting regime under the specific conditions  $U = (N + \frac{1}{2})\omega$ ,  $K_0 = (M + \frac{1}{2})\omega$  ( $N, M$  are integers), and  $\omega \gg J$ . The driving lattice provides the energy quanta  $\omega$  ( $\hbar = 1$ ), which induces the assisted tunneling effect. The effective hopping rates indicate the CDTs by properly modulating the amplitude of the field. We proposed a scheme to realize the directed migration of a strongly correlated particle pair and

considered a scattering model with the interaction between the particle pair and an isolated particle. Their oscillations are utilized to induce a two-partite or even a three-qubit entanglement and reveal the possibility of quantum control, transport, and computing with lattice modulation.

### ACKNOWLEDGMENTS

This work was supported by the NSF of China under Grant No. 11374036 and the National Basic Research Program of China under Grant No. 2012CB821403.

- 
- [1] I. Bloch and W. Zwerger, *Rev. Mod. Phys.* **80**, 885 (2008).  
 [2] I. Bloch, J. Dalibard, and S. Nascimbene, *Nat. Phys.* **8**, 267 (2012).  
 [3] W. S. Bakr, J. I. Gillen, A. Peng, S. Fölling, and M. Greiner, *Nature (London)* **462**, 74 (2009).  
 [4] J. F. Sherson, C. Weitenberg, M. Endres, M. Cheneau, I. Bloch, and S. Kuhr, *Nature (London)* **467**, 68 (2010).  
 [5] M. F. Parsons, F. Huber, A. Mazurenko, C. S. Chiu, W. Setiawan, K. Wooley-Brown, S. Blatt, and M. Greiner, *Phys. Rev. Lett.* **114**, 213002 (2015).  
 [6] D. Jaksch, C. Bruder, J. I. Cirac, C. W. Gardiner, and P. Zoller, *Phys. Rev. Lett.* **81**, 3108 (1998).  
 [7] M. Greiner, O. Mandel, T. Esslinger, T. W. Hänsch, and I. Bloch, *Nature (London)* **415**, 39 (2002).  
 [8] R. Jördens, N. Strohmaier, K. Gnter, H. Moritz, and T. Esslinger, *Nature (London)* **455**, 204 (2008).  
 [9] S. Murmann, A. Bergschneider, V. M. Klinkhamer, G. Zurn, T. Lompe, and S. Jochim, *Phys. Rev. Lett.* **114**, 080402 (2015).  
 [10] M. Aidelsburger, M. Atala, M. Lohse, J. T. Barreiro, B. Paredes, and I. Bloch, *Phys. Rev. Lett.* **111**, 185301 (2013).  
 [11] H. Miyake, G. A. Siviloglou, C. J. Kennedy, W. C. Burton, and W. Ketterle, *Phys. Rev. Lett.* **111**, 185302 (2013).  
 [12] R. N. Palmer, A. Klein, and D. Jaksch, *Phys. Rev. A* **78**, 013609 (2008).  
 [13] A. S. Sørensen, E. Demler, and M. D. Lukin, *Phys. Rev. Lett.* **94**, 086803 (2005).  
 [14] R. N. Palmer and D. Jaksch, *Phys. Rev. Lett.* **96**, 180407 (2006).  
 [15] M. Hafezi, A. S. Sørensen, E. Demler, and M. D. Lukin, *Phys. Rev. A* **76**, 023613 (2007).  
 [16] M. Holthaus and D. W. Hone, *Philos. Mag. B* **74**, 105 (1996).  
 [17] C. Sias, H. Lignier, Y. P. Singh, A. Zenesini, D. Ciampini, O. Morsch, and E. Arimondo, *Phys. Rev. Lett.* **100**, 040404 (2008).  
 [18] D. H. Dunlap and V. M. Kenkre, *Phys. Rev. B* **34**, 3625 (1986).  
 [19] S. Longhi, *J. Phys.: Condens. Matter* **24**, 435601 (2012).  
 [20] F. Grossmann, T. Dittrich, P. Jung, and P. Hanggi, *Phys. Rev. Lett.* **67**, 516 (1991).  
 [21] J. M. Villas-Bôas, S. E. Ulloa, and N. Studart, *Phys. Rev. B* **70**, 041302 (2004).  
 [22] J. Gong, L. Morales-Molina, and P. Hänggi, *Phys. Rev. Lett.* **103**, 133002 (2009).  
 [23] S. Longhi, *Phys. Rev. A* **86**, 044102 (2012).  
 [24] K. Hai, W. Hai, and Q. Chen, *Phys. Rev. A* **82**, 053412 (2010).  
 [25] S. Longhi and G. Della Valle, *Phys. Rev. A* **86**, 043633 (2012).  
 [26] G. Lu, L.-B. Fu, J. Liu, and W. Hai, *Phys. Rev. A* **89**, 033428 (2014).  
 [27] N. Goldman and J. Dalibard, *Phys. Rev. X* **4**, 031027 (2014).  
 [28] D. Y. H. Ho and J. Gong, *Phys. Rev. B* **90**, 195419 (2014).  
 [29] F. Mei, J.-B. You, D.-W. Zhang, X. C. Yang, R. Fazio, S.-L. Zhu, and L. C. Kwek, *Phys. Rev. A* **90**, 063638 (2014).  
 [30] C. E. Creffield, *Phys. Rev. Lett.* **99**, 110501 (2007).  
 [31] C. E. Creffield and G. Platero, *Phys. Rev. B* **69**, 165312 (2004).  
 [32] K. Kudo, T. Boness, and T. S. Monteiro, *Phys. Rev. A* **80**, 063409 (2009).  
 [33] P. M. Preiss, R. Ma, M. E. Tai, A. Lukin, M. Rispoli, P. Zupancic, Y. Lahini, R. Islam, and M. Greiner, *Science* **347**, 1229 (2015).  
 [34] W. S. Dias, M. L. Lyra, and F. A. B. F. de Moura, *Phys. Lett. A* **374**, 4554 (2010).  
 [35] D. Souza and F. Claro, *Phys. Rev. B* **82**, 205437 (2010).  
 [36] R. Khomeriki, D. O. Krimer, M. Haque, and S. Flach, *Phys. Rev. A* **81**, 065601 (2010).  
 [37] G. Corrielli, A. Crespi, G. Della Valle, S. Longhi, and R. Osellame, *Nat. Commun.* **4**, 1555 (2013).  
 [38] Y. Zheng and S.-J. Yang, *New J. Phys.* **18**, 013005 (2016).  
 [39] Á. Rapp, X. Deng, and L. Santos, *Phys. Rev. Lett.* **109**, 203005 (2012).  
 [40] M. Di Liberto, C. E. Creffield, G. I. Japaridze, and C. Morais Smith, *Phys. Rev. A* **89**, 013624 (2014).  
 [41] A. Eckardt, C. Weiss, and M. Holthaus, *Phys. Rev. Lett.* **95**, 260404 (2005).  
 [42] A. Eckardt and M. Holthaus, *Europhys. Lett.* **80**, 50004 (2007).  
 [43] S. Longhi and G. Della Valle, *Phys. Rev. B* **86**, 075143 (2012).  
 [44] S. Greschner, L. Santos, and D. Poletti, *Phys. Rev. Lett.* **113**, 183002 (2014).  
 [45] C. E. Creffield and T. S. Monteiro, *Phys. Rev. Lett.* **96**, 210403 (2006).  
 [46] S. Fölling, S. Trotzky, P. Cheinet, M. Feld, R. Saers, A. Widera, T. Müller, and I. Bloch, *Nature (London)* **448**, 1029 (2007).  
 [47] A. Eckardt, M. Holthaus, H. Lignier, A. Zenesini, D. Ciampini, O. Morsch, and E. Arimondo, *Phys. Rev. A* **79**, 013611 (2009).  
 [48] R. Lohmayer, A. Osterloh, J. Siewert, and A. Uhlmann, *Phys. Rev. Lett.* **97**, 260502 (2006).  
 [49] V. Coffman, J. Kundu, and W. K. Wootters, *Phys. Rev. A* **61**, 052306 (2000).